Charge gap in the one-dimensional dimerized Hubbard model at quarter-filling

Karlo Penc*
Institut de Physique, Université de Neuchâtel, Rue Breguet 1, CH-2000 Neuchâtel, Switzerland

Frédéric Mila
Laboratoire de Physique Quantique, Université Paul Sabatier, 31062 Toulouse, France
(Received 3 June 1994)

We propose a quantitative estimate of the charge gap that opens in the one-dimensional dimerized Hubbard model at quarter-filling due to dimerization, which makes the system effectively half-filled, and to repulsion, which induces umklapp scattering processes. Our estimate is expected to be valid for any value of the repulsion and of the parameter describing the dimerization. It is based on analytical results obtained in various limits (weak coupling, strong coupling, large dimerization) and on numerical results obtained by exact diagonalization of small clusters. We consider two models of dimerization: alternating hopping integrals and alternating on-site energies. The former should be appropriate for the Bechgaard salts, the latter for compounds where the stacks are made of alternating TMTSF and TMTTF molecules.

I. INTRODUCTION

A large number of compounds exhibit one-dimensional electronic properties which can be described by a quarter-filled Hubbard model with some kind of dimerization. For instance, the Bechgaard salts $(TMTSF)_2X$ and $(TMTTF)_2X$, where X denotes an anion such as ClO_4^-, PF_6^-, Br^-, etc., can be regarded concerning their electronic structure as being essentially one-dimensional systems above a crossover temperature T_x of the order of 30 K.[1] From stoichiometry it is known that there are three electrons in the highest occupied molecular orbital (HOMO) for each pair $(TMTSF)_2$, so that the system is $\frac{3}{4}$-filled in terms of electrons or quarter-filled in terms of holes. In the following we will always use hole notation and consider quarter-filled systems. A reasonable description of these properties should be provided by the dimerized Hubbard model defined by the Hamiltonian

$$H = H_0 + H_{\rm int} , \tag{1.1}$$

where the kinetic part of the Hamiltonian is (see Fig. 1)

$$H_0 = -t_1 \sum_{i\ \text{even},\sigma} (c^\dagger_{i,\sigma} c_{i+1,\sigma} + \text{H.c.}) - t_2 \sum_{i\ \text{odd},\sigma} (c^\dagger_{i,\sigma} c_{i+1,\sigma} + \text{H.c.}) . \tag{1.2}$$

The operators $c^\dagger_{i,\sigma}$ create particles in the HOMO of TMTSF or TMTTF with spin σ. We have included two hopping integrals t_1 and t_2 ($t_1 > t_2$) to describe the dimerization along the stacks.[2,3] The dispersion of this model is given by $\varepsilon(k) = \sqrt{t_1^2 + t_2^2 + 2t_1 t_2 \cos k}$ and is depicted in Fig. 2. The important parameters are the dimerization gap $\Delta_D = 2(t_1 - t_2)$ which opens at the Brillouin zone boundary and the total bandwidth $W = 2(t_1 + t_2)$.

To the hopping part of the Hamiltonian we have to add an interaction part to describe the correlation between the electrons. For simplicity, we have chosen the form of the standard Hubbard model

$$H_{\rm int} = U \sum_i n_{i\uparrow} n_{i\downarrow} , \tag{1.3}$$

where U is the on-site Coulomb repulsion and $n_{i,\sigma} = c^\dagger_{i,\sigma} c_{i,\sigma}$.

This model should also provide a good description of salts such as $(FA)_2PF_6$, where FA stands for fluoranthenyl, which is dimerized at room temperature and undergoes a Peierls transition leading to tetramerization along the stacks at a temperature of order 186 K.[4,5] There is another class of materials, however, for which a modified version of the previous model is more appropriate. These materials are related to the Bechgaard salts, but the stacks now consist of alternating TMTTF and TMTSF molecules.[6] A minimal model in this case would

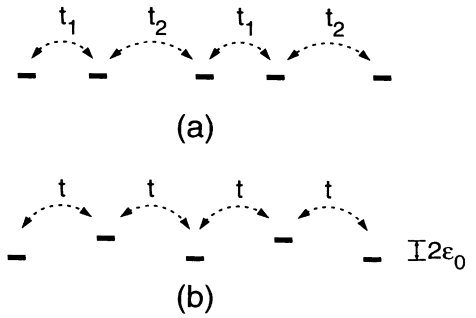

FIG. 1. Schematic representation of the model with (a) alternating hopping amplitudes t_1 and t_2 and (b) alternating on-site energies with energy splitting $2\varepsilon_0$.

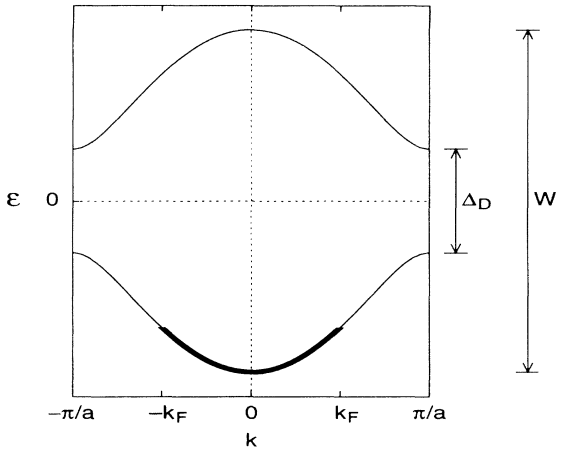

FIG. 2. Band structure of the model with $U = 0$.

be a Hubbard model with alternating atomic on-site energies, with a kinetic part of the form

$$H_0 = -t \sum_{i,\sigma} (c^\dagger_{i,\sigma} c_{i+1,\sigma} + \text{H.c.}) - \varepsilon_0 \sum_{i \text{ even},\sigma} (c^\dagger_{i,\sigma} c_{i,\sigma} - c^\dagger_{i+1,\sigma} c_{i+1,\sigma}) , \quad (1.4)$$

where $2\varepsilon_0$ is the energy splitting between the HOMO of the TMTSF and TMTTF. The dispersion relation is given by $\varepsilon(k) = \sqrt{\varepsilon_0^2 + 2t^2 + 2t^2 \cos k}$. It has the same form as in the previous case. The dimerization gap is now given by $W_D = \sqrt{\varepsilon_0^2 + 4t^2}$ and the bandwidth by $\Delta_D = 2\varepsilon_0$. However, although the dispersion relations are the same, the two models are different because the interaction part will not be the same when expressed in terms of the operators that diagonalize the kinetic part of the Hamiltonian. Let us also note that a similar model has been recently proposed by Sudbø *et al.*[7] as a one-dimensional analog of the copper oxide layers in the high temperature superconductors. A model where dimerization is induced via alternating on-site repulsions has also been studied.[8]

It is clear from Fig. 2 that, due to dimerization, the system is effectively half-filled. In this case, it is known from the general theory of one-dimensional models[9,10] with umklapp scattering that an on-site repulsion of arbitrary size will open a gap in the charge sector. This has been shown explicitly in the case of the Hubbard model for which exact results are available from the Bethe ansatz solution.[11] In the general case, where no exact solution is known, a quantitative estimate of the gap is not available so far. This is unfortunate because such an estimate is necessary to interpret the activated behavior of the resistivity observed at relatively low temperatures in several compounds, which in turn provides an estimate of the magnitude of the Coulomb repulsions. An analysis of that sort has already been performed for the Bechgaard salts of the TMTTF family on the basis of a preliminary determination of the charge gap in the model with alternating hopping amplitudes.[12]

In this paper, we propose a quantitative estimate of the gap in the case of the dimerized models described above that should be valid in the whole range of parameters. This estimate is based on approximations which provide analytical expressions in various limits, and on numerical calculations using Lánczos diagonalization of small clusters. As we think that the results might be useful to readers who do not want to go through the details of the calculation, we start in Sec. II with a detailed account of the results, including analytical expressions, tables, and curves, which can be used independently of the rest of the paper. Then, in Sec. III we explain how and for which values of the parameters numerical estimates can be obtained on the basis of exact diagonalization of small clusters. The following sections are devoted to the approximate expressions that can be obtained analytically in various limits: Sec. IV summarizes exact results in a few trivial limits, Sec. V deals with the large dimerization case, where the dimerization gap is larger than both the repulsion and the Fermi velocity, and Secs. VI and VII deal with the case of weak and strong coupling, respectively. The summary can be found in Sec. II. Throughout the paper, subsections A will deal with the model with alternating hopping amplitudes and subsections B with the model with alternating on-site energies.

II. SUMMARY OF RESULTS

In Fig. 3 we have illustrated the different regimes in which analytical results have been obtained as a func-

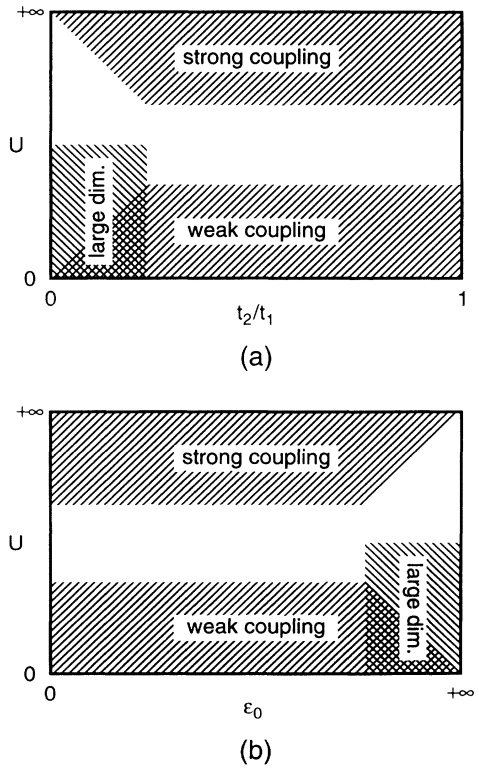

FIG. 3. Schematic picture of the different regions as a function of model parameters for the model with (a) alternating hopping amplitudes and (b) alternating on-site energies.

tion of the model parameters. In this section, we give a summary of these results for each model.

A. Alternating hopping amplitudes

1. Numerical estimates

Using exact diagonalization of small clusters, we have obtained estimates of the charge gap for intermediate values of repulsion U and for $t_2 \leq 0.5t_1$. The limitation comes from the size of the clusters (maximum 16 sites), so that only large gaps corresponding to correlation lengths smaller than 16 sites could be extracted. The numerical results are shown in Fig. 4(a). They are in good agreement with analytical approximations in different limits, as we will show in the subsequent paragraphs.

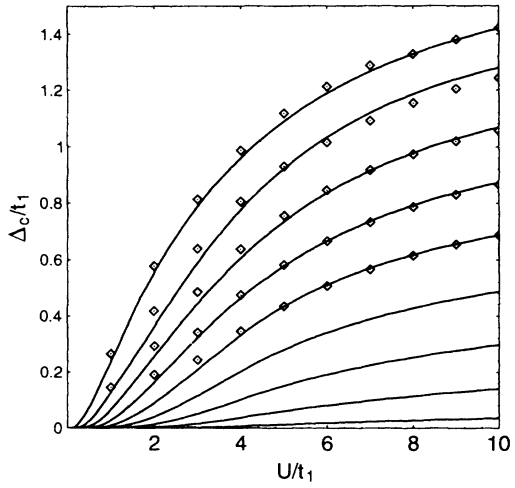

(a)

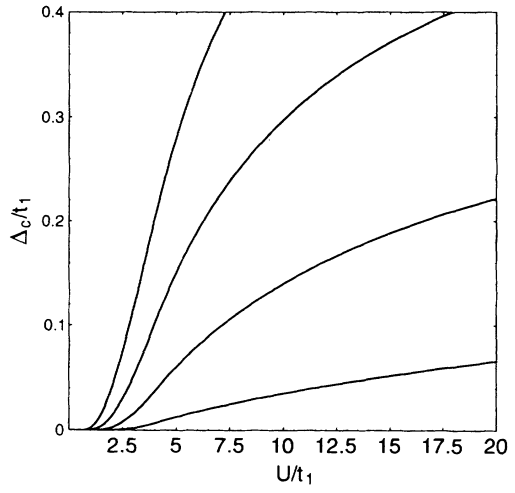

(b)

FIG. 4. (a) Approximation for the charge gap for $t_2/t_1 = 0.1$–0.9 in increments of 0.1 from the top to the bottom. The diamonds are the numerical data for $t_2/t_1 = 0.1$–0.5. (b) Approximation for the gap, but now only for $t_2/t_1 = 0.6$–0.9 in increments of 0.1 from the top to the bottom.

2. Large dimerization

In this limit we have mapped our model onto the exactly solvable Hubbard model at half-filling and we found that the gap is given by

$$\Delta_c = \begin{cases} \dfrac{t_2}{2}\dfrac{8}{\pi}\sqrt{\dfrac{U}{t_2}}e^{-2\pi t_2/U}e^{-\pi t_2/4t_1} & \text{if } t_1 \gg t_2 \gg U \\ \dfrac{U}{2} - \dfrac{U^2}{16t_1} - 2t_2 & \text{if } t_1 \gg U \gg t_2. \end{cases} \tag{2.1}$$

In Fig. 5 we have compared our estimate with numerical results (curve a) for $t_2 = 0.1$, where we can see the crossover from the exponential regime (curve d) to the linear one (curves b and c, b is without the quadratic term $U^2/16t_1$) for $U/t_1 \sim 0.5$.

3. Weak coupling limit

In the weak coupling limit ($U \ll t_1, t_2$), using the renormalization-group (RG) method and results from the large dimerization limit, we found that the gap is exponentially small [see Eq. (6.24)]:

$$\Delta_c = at_1\sqrt{\frac{U}{t_1}}\exp\left(-\frac{bt_1}{U}\right) , \tag{2.2}$$

where the parameters a and b can be found in Table I for different values of t_2/t_1.

In Fig. 6 we compare the numerical values of the gap for $t_2 = 0.3$ and $t_2 = 0.4$ with the weak coupling approximation Eq. (2.2). We can see that up to $U/t_1 = 4$ the weak coupling formula gives very good results.

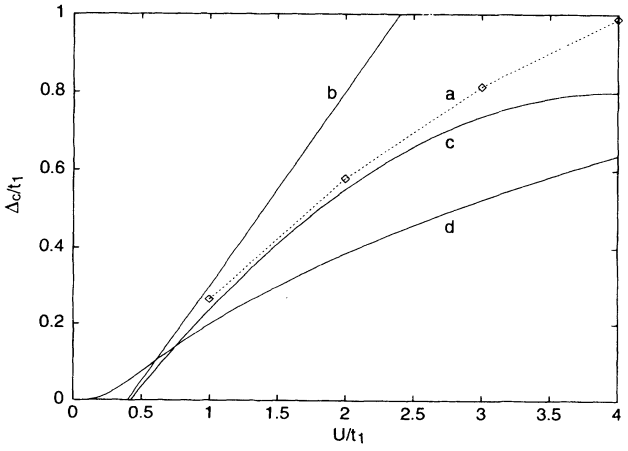

FIG. 5. Numerical estimates of the gap (diamonds) for $t_2 = 0.1$ compared with the analytical results.

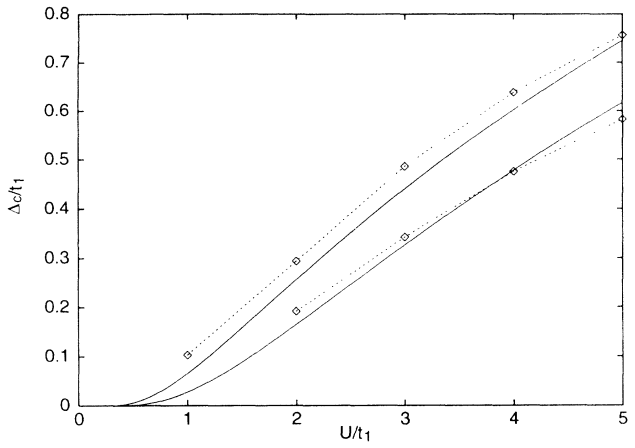

FIG. 6. Weak coupling expression compared to numerical estimates for $t_2 = 0.3$ (upper curve) and $t_2 = 0.4$ (lower curve).

4. *Strong coupling limit*

When the on-site repulsion is large enough ($U \gg t_1, t_2, 4t_1^2/t_2$), the effective Hamiltonian of our model is a $(t-J)$-like Hamiltonian. Applying degenerate perturbation theory, we found that the charge gap is equal to the dimerization gap with a $1/U$ correction [see Eq. (7.20)]:

$$\Delta_c = \Delta_D \left(1 - c\frac{t_1}{U}\right) , \tag{2.3}$$

where the parameters Δ_D/t_1 and c can be found for different values of t_2/t_1 in Table I.

5. *Intermediate region*

On the basis of the previous results, we can propose an estimate of the gap for any value of the parameters. This can be achieved by using Padé approximants to connect the exact results we have obtained for U small and U large, respectively. For $t_2 \geq 0.2$, we have used the weak coupling expression up to U_0, where U_0 is not too large (actually we choose $U_0/t_1 = b$ for $t_2/t_1 \leq 0.5$ and $U_0/t_1 = 4$ for $t_2/t_1 > 0.5$) and Padé approximants of the form

$$f(U) = \frac{a_1 U + \Delta_D U^2}{b_2 + b_1 U + U^2} \tag{2.4}$$

for $U > U_0$. The coefficients are chosen in such a way that, for $U \to +\infty$, the Padé approximant gives the correct large U behavior given by Eq. (2.3) and that, at $U = U_0$, the resulting curve and its derivative be continuous. The curves depend weakly on the value of U_0: Changing the value of U_0 by 50% affects the value of the gap by less then 10%. In Table II we give the values of the coefficients and of U_0 for different values of t_2/t_1.

For $t_2 = 0.1t_1$ we have also used a Padé approximant, but now the limiting behaviors were determined by the second equation in (2.1), which is valid for the intermediate values of U for t_2 small and by Eq. (2.3) in the large U limit. At the crossing point of the weak coupling expression and the Padé approximant, we have eliminated the kink (see Fig. 5) by a linear interpolation. The resulting curves for t_2/t_1 ranging from 0.1 to 0.9 are presented in Fig. 4.

TABLE I. The parameters of the gap equations for the weak coupling and strong coupling limits for the model with alternating hoppings.

t_2/t_1	a	b	Δ_D/t_1	c
0.1	0.36887	0.6336	1.8	1.6816
0.2	0.46782	1.2990	1.6	2.0167
0.3	0.49990	2.0304	1.4	2.3984
0.4	0.48604	2.8669	1.2	2.8368
0.5	0.43672	3.8588	1.0	3.3474
0.6	0.36100	5.0790	0.8	3.9555
0.7	0.26867	6.6518	0.6	4.7075
0.8	0.17046	8.8399	0.4	5.7054
0.9	0.07709	12.4449	0.2	7.2658

TABLE II. The parameters U_0, a_1, b_1, and b_2.

t_2/t_1	U_0/t_1	a_1	b_1	b_2
0.2	1.30	0.45312	1.5438	13.0786
0.3	2.03	-0.13375	1.6173	13.5738
0.4	2.87	-0.97220	1.5540	10.7001
0.5	3.86	-1.91825	1.4287	3.3094
0.6	4	-1.84743	2.6357	0.0736
0.7	4	-1.50580	5.3353	-2.2707
0.8	4	-1.09045	11.5364	-7.4996
0.9	4	-0.60222	33.3189	-34.0969

B. Alternating on-site energies

1. *Large dimerization*

In this limit we have mapped our model to the exactly solvable Hubbard model at half-filling and we found that the gap is given by

$$\Delta_c = \begin{cases} \dfrac{8}{\pi} t \sqrt{\dfrac{U}{2\varepsilon_0}} \exp(-\pi t^2/U\varepsilon_0) & \text{if } \epsilon_0 \gg t \gg U \\ U - \dfrac{2t^2}{\varepsilon_0} & \text{if } \epsilon_0 \gg U \gg t. \end{cases} \tag{2.5}$$

2. *Weak coupling limit*

In the weak coupling limit ($U \ll \varepsilon_0, t$), on the basis of renormalization-group analysis and results from the large dimerization limit, the gap is exponentially small and is given by [see also Eq. (6.38)]

TABLE III. The parameters of the gap equations for the weak coupling and strong coupling limits for the model with alternating on-site energies.

ϵ_0/t	a	b	Δ_D/t	c
0.2	0.60292	8.82123	0.4	5.63087
0.4	0.78553	6.00854	0.8	4.41422
0.6	0.90155	4.53739	1.2	3.71014
0.8	0.97686	3.61670	1.6	3.21882
1	1.02292	2.98899	2	2.84615
2	1.03186	1.56009	4	1.78537
3	0.93780	1.04544	6	1.28117
4	0.84788	0.78494	8	0.99167
5	0.77446	0.62816	10	0.80616

$$\Delta_c = at\sqrt{\frac{U}{t}}\exp\left(-b\frac{t}{U}\right) . \tag{2.6}$$

The parameters a and b are given in Table III for some values of ϵ_0/t.

3. *Strong coupling limit*

When the on-site repulsion is large enough ($U \gg \epsilon_0, t, 4t^2/\epsilon_0$), the effective Hamiltonian of our model is again a $(t-J)$-like Hamiltonian and we found that the charge gap is [see also Eq. (7.36)]

$$\Delta_c = \Delta_D\left(1 - c\frac{t}{U}\right) . \tag{2.7}$$

The parameters Δ_D and c are given in Table III for some values of ϵ_0/t.

III. NUMERICAL SIMULATIONS

We have done intensive numerical simulations based on Lánczos diagonalization of small clusters for the model with alternating hopping integrals. Our numerical estimation for the gap was based on the usual formula

$$\begin{aligned}\Delta_c &= \lim_{N\to+\infty}\Delta_c(N) ,\\ \Delta_c(N) &= E(N+1;2N) + E(N-1;2N)\\ &\quad -2E(N;2N) ,\end{aligned} \tag{3.1}$$

where $E(M;L)$ is the ground state energy for M particles on L sites. We have obtained results for systems of 4, 8, 12, and 16 sites. Periodic (antiperiodic) boundary conditions have been used for $L = 8$ and 16 ($L = 4$ and 12) to have open-shell systems. Typical results are shown in Fig. 7, where we have plotted $\Delta_c(N)$ as a function of $1/N$. Good estimates can be obtained only when the exponential regime $\Delta_c(N) - \Delta_c \sim \exp(-A/N)$, where A is a constant, has been reached for $N = 16$. But the exponential regime is obtained when $v_c/N < \Delta_c$, that is, $N > v_c/\Delta_c$. So we can only obtain good numerical estimates of the gap when Δ_c is not too small, i.e., when U and Δ_D are not too small. The gap can then be extracted by use of the Shanks transformation[13] given by

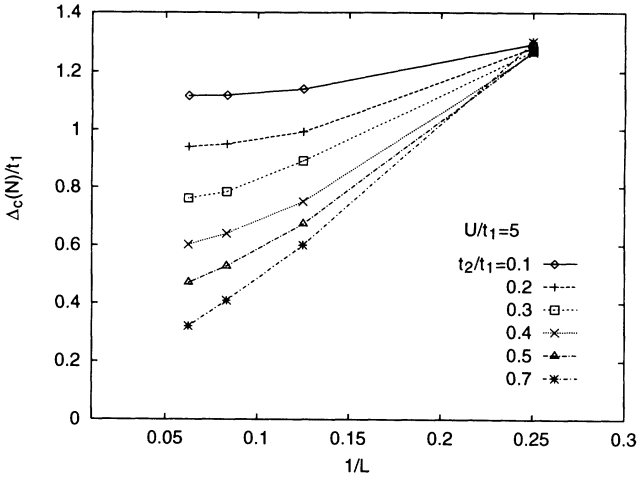

FIG. 7. Numerical values of the gap $\Delta_c(L)$ for $L = 4$, 8, 12, and 16 as a function of $1/L$ for $U/t_1 = 5$. Note that $\Delta_c(L)$ converges very well for small values of t_2/t_1.

$$\Delta_c = \frac{\Delta(N_1)\Delta(N_3) - \Delta(N_2)^2}{\Delta(N_1) + \Delta(N_3) - 2\Delta(N_2)} . \tag{3.2}$$

This procedure has been shown to work very well in the case of the Haldane gap of spin-1 chains.[14] Applying it for $(N_1, N_2, N_3) = (4, 8, 12)$ and $(8, 12, 16)$, respectively gave similar results. The results quoted throughout this paper are those obtained for $(8, 12, 16)$ because they are *a priori* better.

Another limitation comes from the size of the repulsion. When U is very large, the convergence of the Lánczos algorithm becomes very slow and it is no longer possible to get good values of the energy. So, in summary, good estimates have been obtained for $\Delta_D \gtrsim t_1$ and $1 \lesssim U/t_1 \lesssim 60$. This does not cover the range of parameters for actual compounds, for which one often has Δ_D/t_1, or $U/t_1 \ll 1$, and analytical methods are clearly needed to complement these numerical results. In fact, the analytical methods developed in the rest of the paper provide an estimate of the gap for any value of the parameters and the numerical simulations have been only used to check the analytical results.

IV. EXACT RESULTS

A schematic picture of the regions of interest as a function of the model parameters are given in Fig. 3 for each model. Exact, although trivial, results can be deduced on the boundaries and they are summarized in this section.

A. Alternating hopping amplitudes

(i) $t_1 = t_2$. This is a quarter-filled Hubbard model and we know from the Bethe ansatz solution that there is no

gap in the spectrum.

(ii) $t_2 = 0$. The Hamiltonian describes a set of independent systems, each system consisting of two sites. At $\frac{1}{4}$-filling there is one electron for each pair of sites in the ground state. The gap is then given by $\Delta_c = E_0(0) + E_0(2) - 2E_0(1)$, where $E_0(n)$ is the ground state energy of n electron on a pair of sites. These energies are $E_0(0) = 0$, $E_0(1) = -2t_1$, and $E_0(2) = (U - \sqrt{U^2 + 16t_1^2})/2$ and the charge gap is

$$\Delta_c = 2t_1 + \frac{U}{2} - \sqrt{\frac{U^2}{4} + 4t_1^2} = \begin{cases} \dfrac{U}{2} - \dfrac{U^2}{16t_1} & \text{if } t_1 \gg U \\ 2t_1 - \dfrac{4t_1^2}{U} & \text{if } t_1 \ll U. \end{cases} \tag{4.1}$$

(iii) $U = 0$. The band structure is given in Fig. 2. The Fermi energy is in the middle of the lower band, and $\Delta_c = 0$.

(iv) $U = +\infty$. The energies that enter Eq. (3.1) are the same as for free spinless fermions at half-filling, because the energy is independent of the spin when $U = +\infty$ for open boundary conditions (or for periodic one in the limit $N \to +\infty$). So the charge gap is actually the same as for a system of spinless fermions described by the kinetic part of the Hamiltonian at half-filling, which is nothing but the dimerization gap (see Fig. 2). So $\Delta_c = \Delta_D$.

B. Alternating on-site energies

(i) $\varepsilon_0 = 0$. This is a quarter-filled Hubbard model and there is no gap.

(ii) $\varepsilon_0 = +\infty$. The odd sites are outside the Hilbert space. The ground state has one particle per even site and the first excited state has a doubly occupied site. So clearly $\Delta_c = U$.

(iii) $U = 0$. The Fermi energy is in the middle of the band, and $\Delta_c = 0$.

(iv) $U = +\infty$. The dimerization gap $2\varepsilon_0$ and the charge gap coincide, like in the case of alternating hoppings.

(v) In the atomic limit ($t = 0$) the charge gap is given by $\Delta_c = \min(U, 2\varepsilon_0)$.

V. THE LIMIT OF LARGE DIMERIZATION

In this section, we consider the limit of large dimerization, which is the limit where the dimerization gap Δ_D is much larger than both the width of each subband and the repulsion U. This limit corresponds to $t_1 \gg t_2, U$ for the model with alternating hoppings and to $\varepsilon_0 \gg t, U$ for the model with alternating on-site energies. It is particularly interesting because in both cases the model can be mapped onto the half-filled Hubbard model, so that we can use the exact result provided by the Bethe ansatz for the charge gap.[11]

A. Alternating hopping amplitudes

To diagonalize the part of the Hamiltonian corresponding to the hopping terms t_1, we introduce bonding and antibonding operators defined by

$$\begin{aligned} b_{j,\sigma} &= \frac{1}{\sqrt{2}}\left[c_{j,\sigma} + c_{j+1,\sigma}\right], \\ a_{j,\sigma} &= \frac{1}{\sqrt{2}}\left[c_{j,\sigma} - c_{j+1,\sigma}\right], \end{aligned} \tag{5.1}$$

where j is now even. In terms of these operators, the Hamiltonian becomes

$$\begin{aligned} H = &-t_1 \sum_{j \text{ even},\sigma} \left(b^\dagger_{j,\sigma} b_{j,\sigma} - a^\dagger_{j,\sigma} a_{j,\sigma}\right) \\ &-\frac{t_2}{2} \sum_{j \text{ even},\sigma} \Big(b^\dagger_{j,\sigma} b_{j+2,\sigma} + b^\dagger_{j+2,\sigma} b_{j,\sigma} + b^\dagger_{j,\sigma} a_{j+2,\sigma} + a^\dagger_{j+2,\sigma} b_{j,\sigma} \\ &\qquad - a^\dagger_{j,\sigma} b_{j+2,\sigma} - b^\dagger_{j+2,\sigma} a_{j,\sigma} - a^\dagger_{j,\sigma} a_{j+2,\sigma} - a^\dagger_{j+2,\sigma} a_{j,\sigma}\Big) \\ &+\frac{U}{2} \sum_{j \text{ even}} \left[\left(n_{d,j\uparrow} + n_{f,j\uparrow}\right)\left(n_{d,j\downarrow} + n_{f,j\downarrow}\right) + \left(b^\dagger_{j,\uparrow} a_{j,\uparrow} + a^\dagger_{j,\uparrow} b_{j,\uparrow}\right)\left(b^\dagger_{j,\downarrow} a_{j,\downarrow} + a^\dagger_{j,\downarrow} b_{j,\downarrow}\right)\right]. \end{aligned} \tag{5.2}$$

The bonding and the antibonding bands are separated by a large energy $2t_1$. The occupation of the upper band is thus negligible and to zeroth order in $1/t_1$ we get

$$\begin{aligned} H_{\text{eff}} = &-\frac{t_2}{2} \sum_{j \text{ even},\sigma} \left(b^\dagger_{j,\sigma} b_{j+2,\sigma} + \text{H.c.}\right) \\ &+\frac{U}{2} \sum_{j \text{ even}} n_{b,j,\uparrow} n_{b,j,\downarrow} + O(1/t_1), \end{aligned} \tag{5.3}$$

which is nothing but the regular Hubbard model with a repulsion $\tilde{U} = U/2$ and a hopping integral $\tilde{t} = t_2/2$. Here the Hamiltonin acts on a Hilbert space where the antibonding states are all empty. The value of the gap in the half-filled Hubbard model is known exactly from the Bethe ansatz solution. For small interaction ($\tilde{U} \ll \tilde{t}$), it is given by $\Delta_c = (8\tilde{t}/\pi)\sqrt{\tilde{U}/\tilde{t}}\exp(-2\pi\tilde{t}/\tilde{U})$, which, with our notations, reads

$$\Delta_c = \frac{t_2}{2}\frac{8}{\pi}\sqrt{\frac{U}{t_2}}e^{-2\pi t_2/U} . \tag{5.4}$$

For large interaction ($U \gg t_2$ but still $U \ll t_1$), the exact expression becomes $\Delta_c = U/2 - 2t_2$.

To compare with other limits, it is useful to go to next order in $1/t_1$. Using a Schrieffer-Wolff transformation, we can determine the $1/t_1$ corrections to the zeroth order effective Hamiltonian by including scattering processes to the antibonding band and we get

$$\begin{aligned} H_{\text{eff}} = & -\frac{t_2}{2}\sum_{j\ \text{even},\sigma}(b^\dagger_{j,\sigma}b_{j+2,\sigma} + \text{H.c.}) \\ & + \left(\frac{U}{2} - \frac{U^2}{16t_1}\right)\sum_{j\ \text{even}} n_{b,j,\uparrow}n_{b,j,\downarrow} \\ & + \frac{t_2^2}{8t_1}\sum_{j\ \text{even},\sigma}\left(b^\dagger_{j-2,\sigma}b_{j+2,\sigma} + b^\dagger_{j+2,\sigma}b_{j-2,\sigma}\right) \\ & + O(1/t_1^2) . \end{aligned} \tag{5.5}$$

The on-site repulsion is reduced by a $U^2/16t_1$ and a second nearest neighbor hopping appears. The formula for the gap is now modified to

$$\Delta_c = \begin{cases} \dfrac{t_2}{2}\dfrac{8}{\pi}\sqrt{\dfrac{U}{t_2}}e^{-2\pi t_2/U}e^{-\pi t_2/4t_1} & \text{if } U \ll t_2 \\ \dfrac{U}{2} - \dfrac{U^2}{16t_1} - 2t_2 & \text{if } U \gg t_2. \end{cases} \tag{5.6}$$

The second formula agrees with Eq. (4.1) when $t_2 = 0$. The first one will be used in Sec. VI. We have illustrated the above estimates of the gap in Fig. 5.

B. Alternating on-site energies

In the limit $\varepsilon_0 \gg U, t$ the occupation of the energetically lower lying even sites is much larger than that of the odd sites. Using this, we can again find an effective Hamiltonian starting from $t = 0$, in which case only the even sites are occupied. Switching on the hopping, the electrons can hop to the energetically unfavorable odd sites, and from those sites they can hop further. This second order virtual process produces an effective hopping of order $t^2/2\varepsilon_0$ between the even sites, so that the effective Hamiltonian is given by

$$\begin{aligned} H_{\text{eff}} = & -\frac{t^2}{2\varepsilon_0}\sum_{j\ \text{even},\sigma}(c^\dagger_{j,\sigma}c_{j+2,\sigma} + \text{H.c.}) \\ & + U\sum_{j\ \text{even}} n_{j,\uparrow}n_{j,\downarrow} . \end{aligned} \tag{5.7}$$

Here the Hamiltonian acts on a Hilbert space with empty odd sites. This effective Hamiltonian describes a half-filled Hubbard model with a hopping amplitude $\tilde{t} = t^2/2\varepsilon_0$ and repulsion $\tilde{U} = U$, so again we can use the expression of the charge gap for the Hubbard model. In the weak coupling limit ($U \ll t^2/\varepsilon_0$), we get

$$\Delta_c = \frac{8}{\pi}t\sqrt{\frac{U}{2\varepsilon_0}}\exp\left(\frac{-\pi t^2}{U\varepsilon_0}\right) . \tag{5.8}$$

In the intermediate coupling limit, where U is larger than the effective hopping, but smaller than the energy splitting of the two bands ϵ_0, the gap is given by $\Delta_c = U - 2t^2/\varepsilon_0$.

VI. WEAK COUPLING LIMIT

In this limit we can first diagonalize the hopping part of the Hamiltonian and treat the interaction as a perturbation. To do that, we introduce the Fourier transforms of the electron creation and annihilation operators keeping in mind that there are two sites in the unit cell:

$$\begin{aligned} c_{k,\sigma} &= \sqrt{\frac{2}{L}}\sum_{j\ \text{even}} e^{-ikj/2}c_{j,\sigma} , \\ \tilde{c}_{k,\sigma} &= \sqrt{\frac{2}{L}}\sum_{j\ \text{odd}} e^{-ik(j-1)/2}c_{j,\sigma} . \end{aligned} \tag{6.1}$$

Here L is the number of sites, $L/2$ is the number of unit cells, and the length of the unit cell is set to 1.

A. Alternating hopping amplitudes

The Fourier transform of the kinetic part of the Hamiltonian (1.2) is

$$\begin{aligned} H_0 = & -\sum_{k,\sigma}[(t_1 + t_2e^{-ik})c^\dagger_{k,\sigma}\tilde{c}_{k,\sigma} \\ & + (t_1 + t_2e^{ik})\tilde{c}^\dagger_{k,\sigma}c_{k,\sigma}] . \end{aligned} \tag{6.2}$$

Let us introduce annihilation operators for the electrons in the lower ($d_{k,\sigma}$) and upper ($f_{k,\sigma}$) bands by

$$\begin{aligned} d_{k,\sigma} &= \frac{1}{\sqrt{2}}[s(k)c_{k,\sigma} + s^*(k)\tilde{c}_{k,\sigma}] , \\ f_{k,\sigma} &= \frac{1}{\sqrt{2}}[s(k)c_{k,\sigma} - s^*(k)\tilde{c}_{k,\sigma}] , \end{aligned} \tag{6.3}$$

where $s(k) = \exp i(\alpha_k/2 + k/4)$ and α_k is defined by

$$\tan\alpha_k = \frac{t_2 - t_1}{t_2 + t_1}\tan\frac{k}{2} \quad \left(-\frac{\pi}{2} < \alpha_k < \frac{\pi}{2}\right) . \tag{6.4}$$

The hopping part of the Hamiltonian is now diagonal:

$$H_0 = -\sum_{k,\sigma}\varepsilon(k)\left(d^\dagger_{k,\sigma}d_{k,\sigma} - f^\dagger_{k,\sigma}f_{k,\sigma}\right) , \tag{6.5}$$

with

$$\varepsilon(k) = \sqrt{t_1^2 + t_2^2 + 2t_1t_2\cos k} . \tag{6.6}$$

The Fermi velocity v_F is given by

$$v_F = \frac{t_1 t_2}{\sqrt{t_1^2 + t_2^2}} = \frac{1}{8}\frac{W^2 - \Delta_D^2}{\sqrt{(W^2 + \Delta_D^2)/2}} , \tag{6.7}$$

where $\Delta_D = 2(t_1 - t_2)$ is the dimerization gap and $W = 2(t_1 + t_2)$ is the total bandwidth (see Sec. I).

The Fourier transform of the Hamiltonian (1.3) describing the interaction is

$$H_{\rm int} = U\frac{1}{L}\sum_{k_1,k_2,k_3,k_4}\left(c^\dagger_{k_1,\uparrow}c^\dagger_{k_2,\downarrow}c_{k_3,\downarrow}c_{k_4,\uparrow} + \tilde{c}^\dagger_{k_1,\uparrow}\tilde{c}^\dagger_{k_2,\downarrow}\tilde{c}_{k_3,\downarrow}\tilde{c}_{k_4,\uparrow}\right) , \tag{6.8}$$

where $k_1 + k_2 - k_3 - k_4 = Q$ is a vector of the reciprocal lattice. Usually $Q = 0$, but if one of the bands is half-filled, the umklapp processes with $Q = \pm 2\pi$ become important. Using the operators defined by Eq. (6.3), the interaction can be written as

$$H_{\rm int} = \frac{U}{2}\frac{1}{L}\sum_{k_1,k_2,k_3,k_4}\cos\left(\frac{\alpha_{k_1} + \alpha_{k_2} - \alpha_{k_3} - \alpha_{k_4}}{2} + \frac{Q}{4}\right) \times d^\dagger_{k_1,\uparrow}d^\dagger_{k_2,\downarrow}d_{k_3,\downarrow}d_{k_4,\uparrow} , \tag{6.9}$$

where we have kept only the fermions near the Fermi energy.

From the interaction part of the Hamiltonian we can identify the interactions between the electrons near the Fermi surface, the so-called g couplings of the g-ology.[9] Usually these couplings are spin dependent. However, in our model the interaction is isotropic, thus we do not have to worry about the spin dependence; they read

$$g_1 = g_2 = g_4 = \frac{U}{2} ,$$
$$g_3 = -\sin(2\alpha_F)\frac{U}{2} = \frac{\Delta_D}{W}\frac{2}{1 + (\Delta_D/W)^2}\frac{U}{2} . \tag{6.10}$$

The umklapp scattering amplitude g_3 vanishes linearly with Δ_D for small Δ_D/W, in agreement with the estimates[15] obtained using perturbational arguments to get the strength of the umklapp scattering. Clearly, the model of Eq. (6.10) is not equivalent to the half-filled Hubbard model, for which all the g couplings are equal and given by U.

In perturbation theory, the logarithmic corrections to the vertex generate the differential equations of the RG approach when one integrates out the degrees of freedom far from the Fermi level.[9,10] There are four differential equations altogether, but near half-filling we need only the equations which describe the charge degrees of freedom and give rise to the charge gap. As we know from Larkin and Sak,[16] to account correctly for the fluctuations which give rise to the $\sqrt{U}$ factor in Eq. (5.4), we need the RG equations up to third order in the g's. Introducing $g = 2g_2 - g_1$ and denoting by $\tilde{g}$ the renormalized couplings corresponding to momentum cutoff $\tilde{D}$, the third order RG equations we need are

$$\frac{d\tilde{g}}{d\ln\tilde{D}} = -\frac{1}{\pi v_c}\tilde{g}_3^2 + \frac{1}{2\pi^2 v_c^2}\tilde{g}\tilde{g}_3^2 ,$$
$$\frac{d\tilde{g}_3}{d\ln\tilde{D}} = -\frac{1}{\pi v_c}\tilde{g}\tilde{g}_3 + \frac{1}{4\pi^2 v_c^2}\left[\tilde{g}^2\tilde{g}_3 + \tilde{g}_3^3\right] , \tag{6.11}$$

where $v_c = v_F + g_4/2\pi$ is the velocity of the charge excitations. There is a scaling invariant $C = (\tilde{g}^2 - \tilde{g}_3^2)/(2\pi v_c - \tilde{g})$ and the system of equations above can be rewritten as a single differential equation

$$\frac{d\tilde{g}}{d\ln\tilde{D}} = \pi v_c\left(\frac{\tilde{g}^2}{\pi^2 v_c^2} + \frac{C\tilde{g}}{\pi^2 v_c^2} - \frac{2C}{\pi v_c}\right)\left(1 - \frac{\tilde{g}}{2\pi v_c}\right) . \tag{6.12}$$

Reducing the cutoff $\tilde{D}$, we scale towards the strong coupling region, where the RG equations are no longer valid. This crossover occurs when the cutoff $\tilde{D}$ corresponds to an energy scale that has been identified with the charge gap.[10,16,17] So integrating the scaling equations (6.12), we get

$$\int_{\Delta_c/v_c}^{\tilde{D}_0} d\tilde{D}\ln\tilde{D} = -\int_{\tilde{g}(\Delta_c)}^{g}\frac{d\tilde{g}}{\pi v_c}\left(\frac{\tilde{g}^2}{\pi^2 v_c^2} + \frac{C\tilde{g}}{\pi^2 v_c^2} - \frac{2C}{\pi v_c}\right)^{-1} \times\left(1 - \frac{\tilde{g}}{2\pi v_c}\right)^{-1} , \tag{6.13}$$

where $\tilde{D}_0$ is the initial cutoff with $\tilde{g}(\tilde{D}_0) = g$ and $\tilde{g}_3(\tilde{D}_0) = g_3$. Keeping only the leading and next to leading terms of g, and introducing the notation $\xi = g_3/g$, one gets

$$\ln\frac{\Delta_c}{v_c} - \ln\tilde{D}_0 = \frac{1}{2}\ln\frac{\xi g}{\pi v_c} - \left(\frac{\pi v_c}{g} - \frac{1}{4}\right)\frac{\tanh^{-1}\sqrt{1-\xi^2}}{\sqrt{1-\xi^2}} + \frac{1}{4} + \ln C_\Delta , \tag{6.14}$$

where the constant $\ln C_\Delta$ contains terms such as $1/\tilde{g}(\Delta_c)$, which are small compared to $1/g$, as $\tilde{g}$ scales towards the strong coupling limit. Since in that region the RG equations are no longer valid, all the possible corrections are incorporated in that constant.[16] We have separated $1/4$ from the constant $\ln C_\Delta$ for convenience.

Replacing v_c by $v_F + g/2\pi$ ($g_4 = g$ in the leading order in U) and exponentiating, we get

$$\Delta_c = C_\Delta\tilde{D}_0 v_F\sqrt{\frac{\xi g}{\pi v_F}}\exp\left(-\frac{\pi v_F}{g}\frac{\tanh^{-1}\sqrt{1-\xi^2}}{\sqrt{1-\xi^2}}\right) \times\exp\left(-\frac{1}{4}\frac{\tanh^{-1}\sqrt{1-\xi^2}}{\sqrt{1-\xi^2}} + \frac{1}{4}\right) . \tag{6.15}$$

Its behavior in the case of small dimerization is given by

$$\Delta_c = C_\Delta\tilde{D}_0 v_F\sqrt{\frac{2g}{\pi v_F}}e^{1/4}\left(\frac{\xi}{2}\right)^{(\pi v_F/g + 3/4)} , \tag{6.16}$$

where we have used the fact that $\tanh^{-1}\sqrt{1-\xi^2} \approx$

$\ln(2/\xi)$ if $\xi \to 0$. This is the same form as that found by Luther[18] for the charge gap if the umklapp scattering is small compared to the $2g_2 - g_1$, which in our notation means $\xi \ll 1$ (see also Ref. 10).

Using the g couplings of Eq. (6.10) in Eq. (6.15) provides us with the functional dependence of the gap on the repulsion U. This expression also includes a dependence on t_2/t_1. It does *not* give the full dependence on t_2/t_1 however. The reason is the following: Our estimate of the charge gap accounts neither for the curvature of the band (as the RG equations are based on a model with linear dispersion relation) nor for the possible processes involving the empty band. These virtual processes will contribute as higher order corrections in U to the effective interactions near the Fermi surface. Since in the formula for the charge gap these effective couplings appear essentially as $\exp(-\pi v_F/g)$, the U^2 correction to the effective coupling will give an $O(1)$ correction, i.e., if we assume for a moment that $g = U - \gamma U^2 + O(U^3)$, then $1/g = 1/U + \gamma + O(U)$ and $\exp(-\pi v_F/g) = \exp(-\pi v_F \gamma)\exp(-\pi v_F/U)$. So the correction appears as a multiplying factor that depends on t_2/t_1 in the equation for the gap. Clearly, to get a quantitative estimate of the gap one has to include these contributions.

To be fully consistent with our determination of the U dependence, which relies on RG equations up to third order in g [see Eq. (6.11)], one should in principle calculate the vertex corrections to the coupling constants to third order in U. The problem with that program is that the calculation of the third order is hopelessly cumbersome. We think, however, that a calculation of the vertex correction to second order in U is sufficient. The procedure we have used is the following: First, we calculate the second order corrections to the effective interactions near the Fermi surface by integrating out all the electron states except those which are closer to the Fermi surface than some small cutoff $\tilde{D}_0$ in the lower band. Then, if the cutoff $\tilde{D}_0$ is small enough, the dispersion relation of the electrons within this cutoff around the Fermi surface is essentially linear and we can safely use the RG equations of Eq. (6.11) to decrease the cutoff further down to Δ_c/v_c. Now, the cutoff $\tilde{D}_0$ can be taken to be very small: It just has to be larger than Δ_c/v_c and we already know that this quantity is exponentially small in the weak coupling limit. So this procedure should be valid. Finally, we will see that for small $\tilde{D}_0$ ($W/v_c \gg \tilde{D}_0 \gg \Delta_c/v_c$) the result for the gap is independent of the cutoff $\tilde{D}_0$.

To calculate the higher corrections in U, we must take into account the virtual processes that involve states in the upper band and consider the full interaction Hamiltonian instead of Eq. (6.9):

$$H_{\rm int} = \frac{U}{2}\frac{1}{L}\sum_{k_1,k_2,k_3,k_4} \cos\left(\frac{\alpha_{k_1} + \alpha_{k_2} - \alpha_{k_3} - \alpha_{k_4})}{2} + \frac{Q}{4}\right) \times \left(d^\dagger_{k_1,\uparrow} d^\dagger_{k_2,\downarrow} d_{k_3,\downarrow} d_{k_4,\uparrow} + f^\dagger_{k_1,\uparrow} f^\dagger_{k_2,\downarrow} d_{k_3,\downarrow} d_{k_4,\uparrow} + d^\dagger_{k_1,\uparrow} d^\dagger_{k_2,\downarrow} f_{k_3,\downarrow} f_{k_4,\uparrow} + \ldots\right) , \tag{6.17}$$

where we have written only the terms which are responsible for the second order corrections in U. To that order, the effective interactions are given by

$$\begin{aligned} g_1(\tilde{D}_0) &= \frac{U}{2} - \frac{U^2}{4}(D_1 + D_3) , \\ g_2(\tilde{D}_0) &= \frac{U}{2} - \frac{U^2}{4}(D_1 + D_2 + D_3) , \\ g_3(\tilde{D}_0) &= -\sin(2\alpha_F)\frac{U}{2} - \frac{U^2}{4}(D_4 + D_5) , \end{aligned} \tag{6.18}$$

where we have denoted by $D_1, \ldots, D_5$ the diagrams contributing to the effective interaction (see Fig. 8). They are given by

$$D_1 = 2\int_{\pi/2+\tilde{D}_0}^{\pi} \frac{dq}{2\pi}\frac{1}{2\varepsilon_F - 2\varepsilon(q)} + 2\int_0^{\pi/2-\tilde{D}_0} \frac{dq}{2\pi}\frac{1}{2\varepsilon(q) - 2\varepsilon_F} ,$$

$$D_2 = -2\int_0^{\pi/2-\tilde{D}_0} \frac{dq}{2\pi}\frac{\cos^2[\alpha_F - (\alpha_q + \alpha_{\pi-q})/2] + \sin^2[\alpha_F + (\alpha_q + \alpha_{\pi-q})/2]}{\varepsilon(q) - \varepsilon(\pi - q)} ,$$

$$D_3 = 2\int_0^{\pi} \frac{dq}{2\pi}\frac{1}{2\varepsilon_F + 2\varepsilon(q)} ,$$

$$D_4 = 4\int_0^{\pi/2-\tilde{D}_0} \frac{dq}{2\pi}\frac{-\cos[\alpha_F - (\alpha_q + \alpha_{\pi-q})/2]\sin[\alpha_F + (\alpha_q + \alpha_{\pi-q})/2]}{2\varepsilon_F + \varepsilon(q) + \varepsilon(\pi - q)} ,$$

$$D_5 = -4\int_0^{\pi/2} \frac{dq}{2\pi}\frac{-\cos[\alpha_F - (\alpha_q + \alpha_{\pi-q})/2]\sin[\alpha_F + (\alpha_q + \alpha_{\pi-q})/2]}{\varepsilon(q) - \varepsilon(\pi - q)} . \tag{6.19}$$

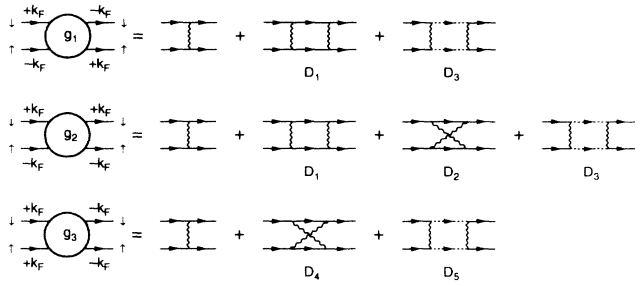

FIG. 8. Perturbational corrections to the effective backward scattering g_1, forward scattering g_2, and umklapp scattering g_3 for the model with alternating hoppings shown up to the second order. The solid (dashed) line represents the fermions in the lower d (upper f) band.

Here α_F and ε_F stand for $\alpha(k_F)$ and $\varepsilon(k_F)$, respectively.

The integrals D_1, D_2, and D_5 contain a logarithmic singularity $\ln(2/\tilde{D}_0)$ and, after some algebra, one can separate these contributions, so that the effective interactions can be written as

$$
\begin{aligned}
g_1(\tilde{D}_0) &= \frac{U}{2} - \frac{U^2}{4}\frac{1}{\pi v_F}\left[\ln\frac{2}{\tilde{D}_0} + \frac{A}{2}I_0^+(A) + O(\tilde{D}_0)\right] , \\
g_2(\tilde{D}_0) &= \frac{U}{2} - \frac{U^2}{4}\frac{1}{\pi v_F}\left\{\frac{1-\sin^2(2\alpha_F)}{2}\ln\frac{2}{\tilde{D}_0}\right. \\
&\quad + \frac{A}{4}\left[I_0^+(A) + I_0^-(A)\right] \\
&\quad - \sin^2(2\alpha_F)\frac{A}{4}\left[I_0^+(A) - I_0^-(A)\right] \\
&\quad \left. - \frac{A}{4}\sin^2(2\alpha_F)I_1(A) + O(\tilde{D}_0)\right\} , \qquad (6.20) \\
g_3(\tilde{D}_0) &= -\sin(2\alpha_F)\left(\frac{U}{2} - \frac{U^2}{4}\frac{1}{\pi v_F}\right. \\
&\quad \times\left\{-\ln\frac{2}{\tilde{D}_0} - \frac{A}{2}\left[I_0^+(A) - I_0^-(A)\right]\right. \\
&\quad \left.\left. - \frac{A}{4}I_1(A) + \frac{A}{2}I_2(A) + O(\tilde{D}_0)\right\}\right) ,
\end{aligned}
$$

where $A = 2t_1t_2/(t_1^2+t_2^2)$ and $I_0^\pm$, I_1, and I_2 are nonsingular integrals given by

$$
\begin{aligned}
I_0^\pm(A) &= \int_0^{\pi/2} d\varphi \frac{1}{1+\sqrt{1\pm A\cos(\varphi)}} , \\
I_1(A) &= \int_0^{\pi/2} d\varphi \left(\frac{1}{\sqrt{1-A\cos(\varphi)}}\right. \\
&\quad \left. - \frac{1}{\sqrt{1+A\cos(\varphi)}}\right) , \qquad (6.21) \\
I_2(A) &= \int_0^{\pi/2} d\varphi \left(1 + \frac{1}{\sqrt{1-A^2\cos^2(\varphi)}}\right) \\
&\quad \times \frac{1}{2+\sqrt{1+A\cos(\varphi)}+\sqrt{1-A\cos(\varphi)}} .
\end{aligned}
$$

For $A \ll 1$, they read

$$
\begin{aligned}
I_0^\pm(A) &= \frac{\pi}{4} \mp \frac{A}{8} + O(A^2) , \\
I_1(A) &= A + O(A^3) , \qquad (6.22) \\
I_2(A) &= \pi/4 + O(A^2) .
\end{aligned}
$$

If it were only for a single band with linear dispersion relation these integrals near the $\ln(2/\tilde{D}_0)$ would not appear.

Using the couplings of Eq. (6.20) in Eq. (6.15), we get

$$
\begin{aligned}
\Delta_c &= 2C_\Delta v_F\sqrt{\frac{2U}{\pi v_F}}(1-A^2)^{1/4}\exp\left(-\frac{2\pi v_F}{U}\frac{\tanh^{-1}A}{A}\right) \\
&\quad \times \exp\left(-\frac{1}{4}\frac{\tanh^{-1}A}{A} + \frac{1}{4}\right) e^{\tilde{C}(A)}[1+O(\tilde{D}_0)] ,
\end{aligned} \qquad (6.23)
$$

where, to first order, $\tilde{D}_0$ disappeared from the expression of the gap. This expression now describes the full functional dependence of Δ_c on U/t_1 and t_2/t_1. The only thing that remains is to determine the prefactor C_Δ. This can be done as follows: From the Bethe ansatz solution of the Hubbard model, we know the value of the gap exactly in the limit of large dimerization [see Eq. (5.4)]. It is easily checked that in the limit $t_2 \to 0$ the functional dependence of Eq. (6.23) is the same as in Eq. (5.4). So we can use the result of Eq. (5.4) to determine the prefactor and this gives $C_\Delta = 2\sqrt{2/\pi}$. Our final expression for the gap in the weak coupling limit is thus

$$
\begin{aligned}
\Delta_c &= \frac{4v_F}{\pi}\sqrt{\frac{U}{v_F}}(1-A^2)^{1/4}\exp\left(-\frac{2\pi v_F}{U}\frac{\tanh^{-1}A}{A}\right) \\
&\quad \times \exp\left(-\frac{1}{4}\frac{\tanh^{-1}A}{A} + \frac{1}{4}\right) e^{\tilde{C}(A)} ,
\end{aligned} \qquad (6.24)
$$

where $A = 2t_1t_2/(t_1^2+t_2^2)$ and $\tilde{C}(A)$ is given by

$$
\begin{aligned}
\tilde{C}(A) &= \frac{1}{4A}\left[2(1-A^2)I_0^-(A) + 2A^2I_0^+(A)\right. \\
&\quad \left. -(1-2A^2)I_1(A) - 2I_2(A)\right] \\
&\quad + \frac{\tanh^{-1}A}{4A^2}\left[-2I_0^-(A) + (1-A^2)I_1(A)\right. \\
&\quad \left. +2(1-A^2)I_2(A)\right] .
\end{aligned} \qquad (6.25)
$$

It is interesting to compare this approach with that of Larkin and Sak,[16] who used slightly different arguments when they calculated the gap in the negative U Hubbard model in the small U limit. It can be shown very easily that our method is equivalent to theirs and gives the same result for the attractive Hubbard model.

B. Alternating on-site energies

The Fourier transform of the kinetic Hamiltonian (1.4) using the Fourier transforms of the operators defined in Eq. (6.1) is

$$H_0 = -\varepsilon_0 \sum_{k,\sigma} \left(c^\dagger_{k,\sigma} c_{k,\sigma} - \tilde{c}^\dagger_{k,\sigma} \tilde{c}_{k,\sigma} \right) - 2t \cos(k/2) \times \sum_{k,\sigma} \left(e^{-ik/2} c^\dagger_{k,\sigma} \tilde{c}_{k,\sigma} + e^{ik/2} \tilde{c}^\dagger_{k,\sigma} c_{k,\sigma} \right) . \quad (6.26)$$

It can be diagonalized in terms of new creation and annihilation operators defined by

$$d_{k,\sigma} = c_{k,\sigma} \cos\beta_k + e^{-ik/2} \tilde{c}_{k,\sigma} \sin\beta_k ,$$
$$f_{k,\sigma} = c_{k,\sigma} \sin\beta_k - e^{-ik/2} \tilde{c}_{k,\sigma} \cos\beta_k , \quad (6.27)$$

where β_k is given by

$$\tan 2\beta_k = \frac{2t}{\varepsilon_0} \cos\frac{k}{2} \quad \left(\frac{-\pi}{4} < \beta_k < \frac{\pi}{4} \right) . \quad (6.28)$$

The kinetic part of the Hamiltonian reads

$$H_0 = -\sum_{k,\sigma} \varepsilon(k) \left(d^\dagger_{k,\sigma} d_{k,\sigma} - f^\dagger_{k,\sigma} f_{k,\sigma} \right) , \quad (6.29)$$

with

$$\varepsilon(k) = \sqrt{\varepsilon_0^2 + 2t^2 + 2t^2 \cos k} . \quad (6.30)$$

The dimerization gap opening at the Brillouin zone boundary is $\Delta_D = 2\varepsilon_0$, the "total" bandwidth is $W = 2\sqrt{\varepsilon_0^2 + 4t^2}$, and the Fermi velocity is

$$v_F = \frac{t^2}{\sqrt{\varepsilon_0^2 + 2t^2}} . \quad (6.31)$$

Replacing the new operators defined in Eq. (6.27) for the lower and upper band into the interaction Hamiltonian (6.8) we get

$$\begin{aligned} H_{\rm int} = U \frac{1}{L} \sum_{k_1,k_2,k_3,k_4} \Big[& (\cos\beta_{k_1} \cos\beta_{k_2} \cos\beta_{k_3} \cos\beta_{k_4} \pm \sin\beta_{k_1} \sin\beta_{k_2} \sin\beta_{k_3} \sin\beta_{k_4}) \, d^\dagger_{k_1,\uparrow} d^\dagger_{k_2,\downarrow} d_{k_3,\downarrow} d_{k_4,\uparrow} \\ & + (\sin\beta_{k_1} \cos\beta_{k_2} \cos\beta_{k_3} \cos\beta_{k_4} \mp \cos\beta_{k_1} \sin\beta_{k_2} \sin\beta_{k_3} \sin\beta_{k_4}) \\ & \times \left(f^\dagger_{k_1,\uparrow} d^\dagger_{k_2,\downarrow} d_{k_3,\downarrow} d_{k_4,\uparrow} + f^\dagger_{k_1,\downarrow} d^\dagger_{k_2,\uparrow} d_{k_3,\uparrow} d_{k_4,\downarrow} + d^\dagger_{k_4,\uparrow} d^\dagger_{k_3,\downarrow} d_{k_2,\downarrow} f_{k_1,\uparrow} + d^\dagger_{k_4,\downarrow} d^\dagger_{k_3,\uparrow} d_{k_2,\uparrow} f_{k_1,\downarrow} \right) \\ & + (\cos\beta_{k_1} \cos\beta_{k_2} \sin\beta_{k_3} \sin\beta_{k_4} \pm \cos\beta_{k_1} \cos\beta_{k_2} \sin\beta_{k_3} \sin\beta_{k_4}) \\ & \times \left(f^\dagger_{k_1,\uparrow} f^\dagger_{k_2,\downarrow} d_{k_3,\downarrow} d_{k_4,\uparrow} + d^\dagger_{k_4,\uparrow} d^\dagger_{k_3,\downarrow} f_{k_2,\downarrow} f_{k_1,\uparrow} \right) + \ldots \Big] , \end{aligned} \quad (6.32)$$

with the constraint $k_1 + k_2 - k_3 - k_4 = Q$ and the upper (lower) signs stand for the normal $Q = 0$ (umklapp $Q = \pm 2\pi$) scattering, respectively. There are altogether 16 terms, but we have kept only the terms which we need to calculate the g's near the Fermi surface up to second order in U.

Like in the case of alternating hopping amplitudes, to determine the effective couplings g, we first integrate out the high energy processes up to some cutoff $\tilde{D}_0$:

$$\begin{aligned} g_1(\tilde{D}_0) &= U(\cos^4\beta_F + \sin^4\beta_F) - U^2 (D_1 + 2D_2 + D_3 + 2D_4) , \\ g_2(\tilde{D}_0) &= U(\cos^4\beta_F + \sin^4\beta_F) - U^2 (D_1 + 2D_2 + D_3 + D_5 + 2D_6) , \\ g_3(\tilde{D}_0) &= U(\cos^4\beta_F - \sin^4\beta_F) - U^2 (2D_7 + D_8 + D_9 + 2D_{10}) , \end{aligned} \quad (6.33)$$

where we have denoted by $D_1, \ldots, D_{10}$ the diagrams contributing to the effective interactions (see Fig. 9), which are given by

$$D_1 = 2 \int_{\pi/2+\tilde{D}_0}^{\pi} \frac{dq}{2\pi} \frac{\left(\cos^2\beta_F \cos^2\beta_q + \sin^2\beta_F \sin^2\beta_q\right)^2}{2\varepsilon_F - 2\varepsilon(q)} + 2 \int_0^{\pi/2-\tilde{D}_0} \frac{dq}{2\pi} \frac{\left(\cos^2\beta_F \cos^2\beta_q + \sin^2\beta_F \sin^2\beta_q\right)^2}{2\varepsilon(q) - 2\varepsilon_F} ,$$

$$D_2 = 2 \int_{\pi/2}^{\pi} \frac{dq}{2\pi} \frac{\left(\cos^2\beta_F \cos\beta_q \sin\beta_q - \sin^2\beta_F \sin\beta_q \cos\beta_q\right)^2}{2\varepsilon_F} ,$$

$$D_3 = 2 \int_0^{\pi} \frac{dq}{2\pi} \frac{\left(\cos^2\beta_F \sin^2\beta_q + \sin^2\beta_F \cos^2\beta_q\right)^2}{2\varepsilon_F + 2\varepsilon(q)} ,$$

$$D_4 = -2 \int_0^{\pi/2} \frac{dq}{2\pi} \frac{\left(\cos^2\beta_F \sin\beta_q \cos\beta_q - \sin^2\beta_F \sin\beta_q \cos\beta_q\right)^2}{2\varepsilon(q)} ,$$

$$D_5 = -2\int_0^{\pi/2-\tilde{D}_0} \frac{dq}{2\pi} \frac{2\cos^4\beta_F\cos^2\beta_q\cos^2\beta_{\pi-q} + 2\sin^4\beta_F\sin^2\beta_q\sin^2\beta_{\pi-q}}{\varepsilon(q)-\varepsilon(\pi-q)} ,$$

$$D_6 = -\int_0^{\pi/2} \frac{dq}{2\pi} \frac{2\cos^4\beta_F\cos^2\beta_q\sin^2\beta_{\pi-q} + 2\sin^4\beta_F\sin^2\beta_q\cos^2\beta_{\pi-q}}{\varepsilon(q)+\varepsilon(\pi-q)} ,$$

$$D_7 = 2\int_{\pi/2}^{\pi} \frac{dq}{2\pi} \frac{\cos^4\beta_F\cos^2\beta_q\sin^2\beta_{\pi-q} - \sin^4\beta_F\sin^2\beta_q\cos^2\beta_{\pi-q}}{2\varepsilon_F-\varepsilon(q)+\varepsilon(\pi-q)} ,$$

$$D_8 = 2\int_0^{\pi} \frac{dq}{2\pi} \frac{\cos^4\beta_F\sin^2\beta_q\sin^2\beta_{\pi-q} - \sin^4\beta_F\cos^2\beta_q\cos^2\beta_{\pi-q}}{2\varepsilon_F+\varepsilon(q)+\varepsilon(\pi-q)} .$$

$$D_9 = -4\int_0^{\pi/2-\tilde{D}_0} \frac{dq}{2\pi} \frac{\cos^4\beta_F\cos^2\beta_q\cos^2\beta_{\pi-q} - \sin^4\beta_F\sin^2\beta_q\sin^2\beta_{\pi-q}}{\varepsilon(q)-\varepsilon(\pi-q)} ,$$

$$D_{10} = -2\int_0^{\pi/2} \frac{dq}{2\pi} \frac{\cos^4\beta_F\cos^2\beta_q\sin^2\beta_{\pi-q} - \sin^4\beta_F\sin^2\beta_q\cos^2\beta_{\pi-q}}{\varepsilon(q)+\varepsilon(\pi-q)} . \tag{6.34}$$

Again, like for the case of alternating hoppings, we separate the logarithmic divergencies from integrals D_1, D_5, and D_9 and we write the effective couplings as

$$g_1(\tilde{D}_0) = \frac{\varepsilon_0^2+t^2}{\varepsilon_0^2+2t^2}U - \frac{U^2}{\pi v_F}\left[\left(\frac{\varepsilon_0^2+t^2}{\varepsilon_0^2+2t^2}\right)^2 \ln\frac{2}{\tilde{D}_0} + I_1\right] ,$$

$$g_2(\tilde{D}_0) = \frac{\varepsilon_0^2+t^2}{\varepsilon_0^2+2t^2}U - \frac{U^2}{\pi v_F}\left(\frac{1}{2}\frac{t^4}{(\varepsilon_0^2+2t^2)^2}\ln\frac{2}{\tilde{D}_0} + \tilde{I}_2\right) ,$$

$$g_3(\tilde{D}_0) = \frac{\varepsilon_0}{\sqrt{\varepsilon_0^2+2t^2}}U - \frac{U^2}{\pi v_F}\left[-\frac{\varepsilon_0(\varepsilon_0^2+t^2)}{(\varepsilon_0^2+2t^2)^{3/2}}\ln\frac{2}{\tilde{D}_0} + \tilde{I}_3\right] . \tag{6.35}$$

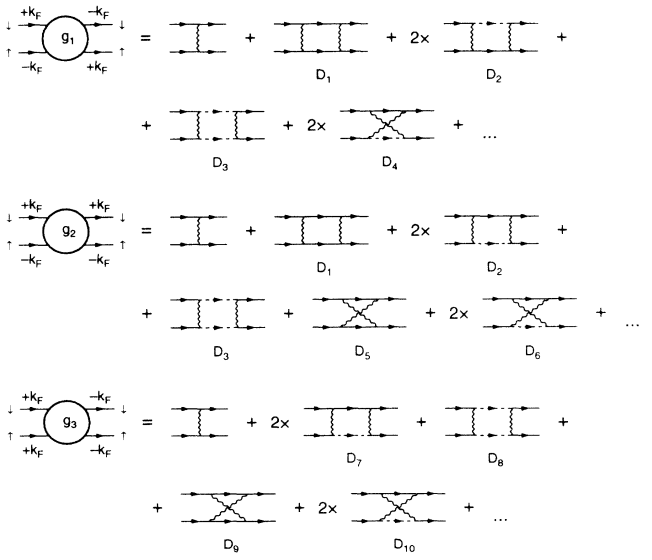

FIG. 9. Perturbational corrections to the effective backward scattering g_1, forward scattering g_2, and umklapp scattering g_3 for the model with alternating hoppings shown up to the second order. The solid (dashed) line represents the fermions in the lower d (upper f) band.

The expressions for the $\tilde{I}$'s are rather complicated and, for brevity, we will give here only their value in the limit of large dimerization (the compounds which can be described by this model presumably have parameters which lie in this limit):

$$\tilde{I}_1 = \frac{32+13\pi}{32}\frac{t^6}{\varepsilon_0^6} + O(t^8/\varepsilon_0^8) ,$$

$$\tilde{I}_2 = \frac{t^4}{4\varepsilon_0^4} - \frac{48+3\pi}{32}\frac{t^6}{\varepsilon_0^6} + O(t^8/\varepsilon_0^8) , \tag{6.36}$$

$$\tilde{I}_3 = \frac{t^2}{4\varepsilon_0^4} - \frac{48+5\pi}{32}\frac{t^6}{\varepsilon_0^6} + O(t^8/\varepsilon_0^8) .$$

We have calculated numerically the $\tilde{I}$'s for a few values of ε_0/t and they are presented in Table IV.

For g_4, it is sufficient to take the value without the U^2 corrections:

$$g_4 = U\frac{\varepsilon_0^2+t^2}{\varepsilon_0^2+2t^2} . \tag{6.37}$$

Replacing the effective interactions into Eq. (6.15), we get

TABLE IV. The $\tilde{I}$'s for some values of ε_0/t.

ε_0/t	$\tilde{I}_1$	$\tilde{I}_2$	$\tilde{I}_3$
0	$\frac{1}{8}\ln 2$	0	0
0.2	0.0832216	0.0007691	0.0020951
0.4	0.0739705	0.0026394	0.0039468
0.6	0.0613605	0.0046787	0.0053306
0.8	0.0480877	0.0061374	0.0061143
1	0.0360938	0.0067624	0.0063123
2	0.0066400	0.0038914	0.0035338
3	0.0013135	0.0015298	0.0014380
4	0.0003309	0.0006442	0.0006189
5	0.0001034	0.0003044	0.0002961

$$\Delta_c = \frac{8}{\pi} t \sqrt{\frac{U\varepsilon_0}{2(\varepsilon_0^2+2t^2)}} \times \exp\left(-\frac{\pi}{U}\sqrt{\varepsilon_0^2+2t^2}\tanh^{-1}\frac{t^2}{\varepsilon_0^2+t^2}\right) \times \exp\left[\frac{1}{4}-\frac{t^2+\varepsilon_0^2}{4t^2}\tanh^{-1}\frac{t^2}{\varepsilon_0^2+t^2}\right] e^{\tilde{C}} , \quad (6.38)$$

where the constant has been fixed so that for large dimerization ($\varepsilon_0 \gg t$) we get Eq. (5.8). Here $\tilde{C}$ is given by

$$\tilde{C} = (2\tilde{I}_2 - \tilde{I}_1)\frac{(2t^2+\varepsilon_0^2)^2}{t^4}\left[1-\frac{t^2+\varepsilon_0^2}{t^2}\tanh^{-1}\frac{t^2}{\varepsilon_0^2+t^2}\right] -\tilde{I}_3\frac{(2t^2+\varepsilon_0^2)^{3/2}}{t^2\varepsilon_0}\left[\frac{\varepsilon_0^2+t^2}{t^2} -\frac{\varepsilon_0^2(2t^2+\varepsilon_0^2)}{t^4}\tanh^{-1}\frac{t^2}{\varepsilon_0^2+t^2}\right] . \quad (6.39)$$

VII. LARGE U LIMIT

In the large U limit a canonical transformation can be applied to obtain an effective Hamiltonian analog to the $t-J$ Hamiltonian of the nondimerized Hubbard model. We know already that if there are two alternating hoppings, a dimerization gap Δ_D opens at the Brillouin zone boundary and in the limit $U \to +\infty$ this gap becomes the charge gap. This will be modified by the spin interaction, which will give corrections of order $1/U$.

A. Alternating hoppings

If $U \gg t_1, t_2$, and since we have two different hopping amplitudes, the effective model will be a $t-J$ model with alternating t_1 and t_2 hoppings and alternating J_1 and J_2 exchange interactions:

$$H_{tJ} = -t_1 \sum_{i\ \mathrm{even},\sigma} \tilde{\mathcal{P}}(c^\dagger_{i,\sigma}c_{i+1,\sigma} + \mathrm{H.c.})\tilde{\mathcal{P}} - t_2 \sum_{i\ \mathrm{odd},\sigma} \tilde{\mathcal{P}}(c^\dagger_{i,\sigma}c_{i+1,\sigma} + \mathrm{H.c.})\tilde{\mathcal{P}} + J_1 \sum_{i\ \mathrm{even}} (S_iS_{i+1} - \tfrac{1}{4}n_in_{i+1}) + J_2 \sum_{i\ \mathrm{odd}} (S_iS_{i+1} - \tfrac{1}{4}n_in_{i+1}) + \frac{J}{4}\sum_{i,\sigma} \tilde{\mathcal{P}}(c^\dagger_{i,\sigma}c^\dagger_{i+1,-\sigma}c_{i+1,\sigma}c_{i+2,-\sigma} - c^\dagger_{i,\sigma}c^\dagger_{i+1,-\sigma}c_{i+1,-\sigma}c_{i+2,\sigma} + \mathrm{H.c.})\tilde{\mathcal{P}} + O(t^3/U^2) . \quad (7.1)$$

Here the projector $\tilde{\mathcal{P}} = \prod_i [1-n_{i,\uparrow}n_{i,\downarrow}]$ ensures that there are no doubly occupied sites $n_i = n_{i,\uparrow}+n_{i,\downarrow}$ and the generated exchange couplings are $J_1 = 4t_1^2/U$, $J_2 = 4t_2^2/U$, and $J = 4t_1t_2/U$.

To go further, let us follow the scheme developed by Shiba and Ogata in their study of the correlation functions for the large U Hubbard model.[19] The basic idea is to treat the exchange part as a perturbation. This is possible if the exchange integrals are smaller than the hopping integrals, which reduces to the condition $J_1 \ll t_2$ (remember that $t_2 < t_1$ and thus that $J, J_2 < J_1$) or, in terms of the original parameters, $U \gg 4t_1^2/t_2$. In this limit, the part describing essentially hopping of spinless fermions can be solved exactly and the exchange part is then treated as a perturbation. This can be achieved by assuming that the wave function is the product of a charge and a spin wave function, where the spin wave function is defined in a Hilbert space of dimension 2^N, i.e., every charge has the additional freedom of having its spin up or down:

$$|\Psi\rangle = |sf\rangle \otimes |\Phi\rangle . \quad (7.2)$$

Here $|\Phi\rangle$ is the spin part of the wave function, while $|sf\rangle$, the wave function of the N spinless fermions, is the ground state of the kinetic Hamiltonian. Following standard perturbation technique for the case of a degenerate ground state, we will have to diagonalize the following $2^N \times 2^N$ Hamiltonian to lift the degeneracy of $|\Phi\rangle$ and get the $1/U$ energy corrections:

$$\langle H_{tJ}\rangle'/L = -t_1\langle c_0^\dagger c_1\rangle' - t_2\langle c_1^\dagger c_2\rangle' + \left(\frac{J_1}{2}\langle n_0n_1\rangle' + \frac{J_2}{2}\langle n_1n_2\rangle' - J\langle c_0^\dagger c_1^\dagger c_1c_2\rangle'\right) \times \frac{1}{N}\sum_{j=1}^{N}(S_jS_{j+1} - \tfrac{1}{4}) , \quad (7.3)$$

where the $\langle\hat{A}\rangle'$ denotes the expectation value of the operator $\hat{A}$ in the Fermi sea of spinless fermions, i.e., $\langle\hat{A}\rangle' = \langle sf|\hat{A}|sf\rangle$.

Before we continue with the calculation of the gap, we need to know the expectation values of electron operators in the Fermi sea of spinless fermions, where $k_{F,\mathrm{SF}} = 2k_F$. Using the translational symmetry of the system, it is enough to calculate the following basic expectation values:

$$\langle c_0^\dagger c_j\rangle' = \frac{2}{L}\sum_k e^{ikj/2}\langle c_k^\dagger c_k\rangle' ,$$
$$\langle c_1^\dagger c_{j+1}\rangle' = \frac{2}{L}\sum_k e^{ikj/2}\langle \tilde{c}_k^\dagger \tilde{c}_k\rangle' , \tag{7.4}$$
$$\langle c_1^\dagger c_j\rangle' = \frac{2}{L}\sum_k e^{ikj/2}\langle \tilde{c}_k^\dagger c_k\rangle' ,$$

where j is even everywhere. More complicated expressions can be calculated by using Wick's theorem, i.e., by constructing all possible pairings. For example:

$$\begin{aligned}\langle n_1 n_j\rangle' &= \langle c_1^\dagger c_1\rangle'\langle c_j^\dagger c_j\rangle' - \langle c_1^\dagger c_j\rangle'\langle c_j^\dagger c_1\rangle' \\ &= n^2 - \langle c_1^\dagger c_j\rangle'^2 , \\ \langle c_0^\dagger c_1^\dagger c_1 c_2\rangle' &= n\langle c_0^\dagger c_2\rangle' - \langle c_0^\dagger c_1\rangle'\langle c_1^\dagger c_2\rangle' .\end{aligned} \tag{7.5}$$

In the following, the sums above will be replaced by integrals

$$\frac{2}{L}\sum_k \to \frac{1}{2\pi}\int_{-\pi}^{\pi} dk . \tag{7.6}$$

The free fermion Hamiltonian (6.2) has been solved in Sec. VI. Using the diagonal electron operators d and f defined in Eq. (6.3), we get

$$\langle c_k^\dagger c_k\rangle' = \langle \tilde{c}_k^\dagger \tilde{c}_k\rangle' = \frac{1}{2}(n_{d,k} + n_{f,k}) ,$$
$$\langle \tilde{c}_k^\dagger c_k\rangle' = \frac{s^{*2}(k)}{2}(n_{d,k} - n_{f,k}) , \tag{7.7}$$

where $n_{d,k} = d_k^\dagger d_k$, similarly for $n_{f,k}$, and the spin index of the fermion operators has been dropped. For j even, this gives

$$\begin{aligned}\langle c_0^\dagger c_j\rangle' = \langle c_1^\dagger c_{j+1}\rangle' &= \frac{1}{2\pi}\int_{-\pi}^{\pi} dk e^{ikj/2}\frac{1}{2}(n_{b,k} + n_{f,k}) \\ &= \frac{\sin \pi j n}{\pi j} .\end{aligned} \tag{7.8}$$

This is the same expression as for a nondimerized model. For $\langle c_1^\dagger c_j\rangle'$, we get

$$\langle c_1^\dagger c_j\rangle' = \frac{1}{2\pi}\int_0^{2\varphi_0} dk \cos[k(j-1)/2 - \alpha_k] , \tag{7.9}$$

where α_k is defined in Eq. (6.4) and

$$\varphi_0 = \begin{cases} \pi n & \text{if } n < 1/2 \\ \pi(1-n) & \text{if } n > 1/2. \end{cases} \tag{7.10}$$

After some algebra, we get

$$\langle c_1^\dagger c_j\rangle' = \frac{1}{\pi}\int_0^{\varphi_0} d\varphi \frac{t_1\cos\varphi j + t_2\cos\varphi(j-2)}{\sqrt{t_1^2 + t_2^2 + 2t_1 t_2\cos 2\varphi}} . \tag{7.11}$$

For $j = 0$ and $j = 2$, this can be written

$$\langle c_1^\dagger c_0\rangle' = \frac{1}{2\pi t_1}\left[(t_1 - t_2)F(\varphi_0, q) + (t_1 + t_2)E(\varphi_0, q)\right] ,$$
$$\langle c_1^\dagger c_2\rangle' = \frac{1}{2\pi t_2}\left[(t_2 - t_1)F(\varphi_0, q) + (t_1 + t_2)E(\varphi_0, q)\right] , \tag{7.12}$$

where we have introduced the notation

$$q = \frac{2\sqrt{t_1 t_2}}{t_1 + t_2} \tag{7.13}$$

and where the elliptic integrals $E(\varphi_0, q)$ and $F(\varphi_0, q)$ are defined by

$$F(\varphi_0, q) = \int_0^{\varphi_0} \frac{d\varphi}{\sqrt{1 - q^2\sin\varphi^2}} ,$$
$$E(\varphi_0, q) = \int_0^{\varphi_0} d\varphi\sqrt{1 - q^2\sin\varphi^2} . \tag{7.14}$$

Now, let us turn back to the effective Hamiltonian (7.3). For the spin degrees of freedom, we are left with an N-site Heisenberg Hamiltonian with an effective exchange interaction $J_{\rm eff}$, which we can read from Eq. (7.3):

$$\begin{aligned}J_{\rm eff} &= \frac{J_1}{2}\langle n_0 n_1\rangle' + \frac{J_2}{2}\langle n_1 n_2\rangle' - J\langle c_0^\dagger c_1^\dagger c_1 c_2\rangle' \\ &= \frac{2}{U}\left[n^2(t_1^2 + t_2^2) - n t_1 t_2\frac{\sin 2\pi n}{\pi}\right. \\ &\quad \left. - \frac{(t_1 - t_2)^2}{\pi^2}F^2(\varphi_0, q)\right] ,\end{aligned} \tag{7.15}$$

where we have used Eqs. (7.5) and (7.12)

In the ground state of the AF Heisenberg model the expectation value $\langle\Phi|(S_0 S_1 - \frac{1}{4})|\Phi\rangle$ is $-\ln 2$ in zero magnetic field, as shown by Griffiths.[20] The energy per site $\langle\Psi|H_{tJ}|\Psi\rangle/L$ is then

$$\varepsilon_{tJ} = \varepsilon_{\rm SF} - J_{\rm eff}\ln 2 , \tag{7.16}$$

where $\varepsilon_{\rm SF} = -t_1\langle c_1^\dagger c_0\rangle' - t_2\langle c_1^\dagger c_2\rangle'$ is the kinetic energy of the spinless fermions per site. From Eq. (7.12), we get

$$\varepsilon_{\rm SF}(n) = -\frac{t_1 + t_2}{\pi}E(\varphi_0, q) , \tag{7.17}$$

which in the nondimerized case ($q = 1$) gives the correct energy $(2t/\pi)\sin\pi n$. For $n = 1/2$, we get

$$J_{\rm eff} = \frac{2}{U}\left[\frac{t_1^2 + t_2^2}{4} - \frac{(t_1 - t_2)^2}{\pi^2}K^2(q)\right] , \tag{7.18}$$

where $K(q) = F(\pi/2, q)$ is the complete elliptic integral defined in Eq. (7.14).

The energy E_{tJ}/L has a cusp as a function of filling at $n = 1/2$ and this nonanaliticity comes from the φ_0 [see Eq. (7.10)]. Therefore the first derivative of E_{tJ}/L has a jump at quarter filling, which is nothing but the charge gap

$$\Delta_c = \left.\frac{\partial \varepsilon_{tJ}}{\partial n}\right|_{n=1/2+0} - \left.\frac{\partial \varepsilon_{tJ}}{\partial n}\right|_{n=1/2-0} . \tag{7.19}$$

In our case this gives

$$\Delta_c = 2(t_1 - t_2)\left[1 - \frac{4\ln 2}{\pi}\frac{t_1+t_2}{U}K\left(\frac{2\sqrt{t_1 t_2}}{t_1+t_2}\right)\right] , \tag{7.20}$$

where we have used the following identities:

$$\left.\frac{\partial F(\varphi_0,q)}{\partial n}\right|_{n=1/2+0} - \left.\frac{\partial F(\varphi_0,q)}{\partial n}\right|_{n=1/2-0} = -\frac{2\pi}{\sqrt{1-q^2}} , \tag{7.21}$$

$$\left.\frac{\partial E(\varphi_0,q)}{\partial n}\right|_{n=1/2+0} - \left.\frac{\partial E(\varphi_0,q)}{\partial n}\right|_{n=1/2-0} = -2\pi\sqrt{1-q^2} .$$

Using the limiting behavior of the elliptic function $K(q) = \ln(4/\sqrt{1-q^2})$, the gap in the small dimerization limit is

$$\Delta_c = 2(t_1 - t_2)\left[1 - \frac{4\ln 2}{\pi}\frac{t_1+t_2}{U}\ln\frac{4(t_1+t_2)}{t_1-t_2}\right] \tag{7.22}$$

or

$$\Delta_c = \Delta_D\left[1 - \frac{2\ln 2}{\pi}\frac{W}{U}\ln\frac{4W}{\Delta_D}\right] . \tag{7.23}$$

In Fig. 10 we have compared the analytical results presented above with the numerical data. The agreement is already very good at $U/t_1 = 10$ for t_2/t_1 between 0.3 and 0.5. To get such a good agreemnt for $t_2/t_1 = 0.1$, one has to go to larger values of U, so that the condition $U \gg 4t_1^2/t_2 \approx 40$ is satisfied. For large values of t_2, the gap is small and the numerical estimate is not accurate.

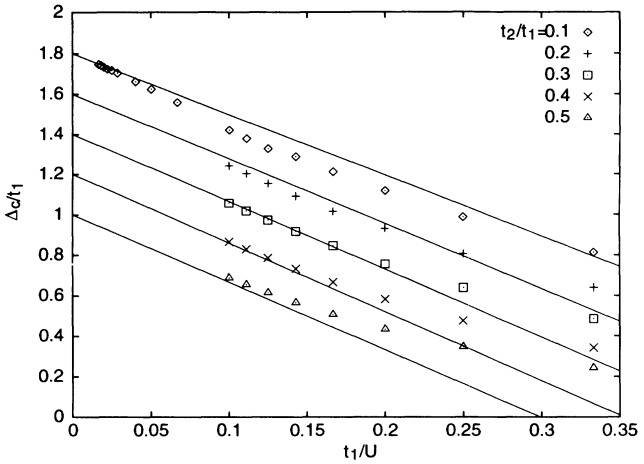

FIG. 10. Numerical estimates of the gap in the large U limit (diamonds) together with the analytical approximation. The results presented are for t_2 =0.1, 0.2, 0.3, 0.4, 0.5, and 0.7 from the top to the bottom.

As $t_2 \to 0$, Eq. (7.20) gives $\Delta_c = 2t_1 - (4\ln 2)t_1^2/U$, in apparent contradiction with the second of equations (4.1), which gives $\Delta_c = 2t_1 - 4t_1^2/U$ for $t_2 = 0$. The origin of the discrepancy is that Eq. (7.20) holds if $U \gg t_1^2/t_2$, while the second of equations (4.1) requires that $t_2 \ll t_1^2/U$. These conditions are clearly incompatible. Actually the crossover between these two regimes can be observed on Fig. 10, where the points below the solid line ($t_1^2/U \approx 0.1$) gives $\Delta_c \sim 2t_1 - 4t_1^2/U$, while for larger values of U we get the correct $4\ln 2$ slope.

B. Alternating on-site energies

Like in the previous case, a canonical transformation can be applied in the limit $U \gg t, \epsilon_0$ to obtain a $(t-J)$-like effective Hamiltonian

$$H_{tJ} = -t\sum_{i,\sigma}\tilde{\mathcal{P}}(c^\dagger_{i,\sigma}c_{i+1,\sigma} + \text{H.c.})\tilde{\mathcal{P}} - \varepsilon_0\sum_{i\ \text{even},\sigma}(c^\dagger_{i,\sigma}c_{i,\sigma} - c^\dagger_{i+1,\sigma}c_{i+1,\sigma}) + J\sum_i(S_iS_{i+1} - \tfrac{1}{4}n_in_{i+1})$$
$$+\frac{J}{4}\sum_{i,\sigma}\tilde{\mathcal{P}}(c^\dagger_{i,\sigma}c^\dagger_{i+1,-\sigma}c_{i+1,\sigma}c_{i+2,-\sigma} - c^\dagger_{i,\sigma}c^\dagger_{i+1,-\sigma}c_{i+1,-\sigma'}c_{i+2,\sigma} + \text{H.c.})\tilde{\mathcal{P}} + O(t^3/U^2) , \tag{7.24}$$

where the projector $\tilde{\mathcal{P}} = \prod_i[1 - n_{i,\uparrow}n_{i,\downarrow}]$ ensures that there are no doubly occupied sites and the generated exchange coupling is $J = 4t^2/U$. If the additional condition $J \ll \epsilon_0$ is satisfied (that is, if $U \gg 4t^2/\epsilon_0$), we can again follow Ogata and Shiba.

Let us now calculate the expectation values for this model. The free fermion model is given by Eq. (6.26) and it has been solved using transformations Eq. (6.27). So, for the expectation values we get

$$\langle c^\dagger_k c_k\rangle' = \frac{n_{d,k}+n_{f,k}}{2} + \frac{n_{d,k}-n_{f,k}}{2}\cos 2\beta_k ,$$
$$\langle \tilde{c}^\dagger_k \tilde{c}_k\rangle' = \frac{n_{d,k}+n_{f,k}}{2} - \frac{n_{d,k}-n_{f,k}}{2}\cos 2\beta_k , \tag{7.25}$$
$$\langle \tilde{c}^\dagger_k c_k\rangle' = e^{-ik/2}\frac{n_{d,k}-n_{f,k}}{2}\sin 2\beta_k ,$$
$$\langle c^\dagger_k \tilde{c}_k\rangle' = e^{ik/2}\frac{n_{d,k}-n_{f,k}}{2}\sin 2\beta_k .$$

Using the results we obtained in Eq. (7.8), for j even we get

$$\langle c_0^\dagger c_j\rangle' = \frac{\sin \pi jn}{\pi j} + I_j \ , \qquad \langle c_1^\dagger c_{j+1}\rangle' = \frac{\sin \pi jn}{\pi j} - I_j \ , \tag{7.26}$$

and after some algebra

$$\langle c_0^\dagger c_{j-1}\rangle' = \langle c_1^\dagger c_j\rangle' = \frac{t}{\varepsilon_0}(I_j + I_{j-2}) \ , \tag{7.27}$$

where the I_j denote the following integral:

$$I_j = \frac{1}{2}\frac{1}{2\pi}\int_{2\varphi_0}^{2\varphi_0} dk e^{ikj/2}\cos 2\beta_k = \frac{1}{2\pi}\int_0^{2\varphi_0} dk \frac{\cos(kj/2)}{\sqrt{1+(2t/\varepsilon_0)^2\cos^2(k/2)}} \tag{7.28}$$

and φ_0 is defined by Eq. (7.10). These are elliptic integrals and, e.g., I_0 and I_2 are given by

$$I_0 = \frac{1}{\pi}\frac{\varepsilon_0}{\sqrt{\varepsilon_0^2+4t^2}}F(\varphi_0,q) \ , \qquad I_0 - I_2 = \frac{2}{\pi}\frac{\varepsilon_0\sqrt{\varepsilon_0^2+4t^2}}{4t^2}\left[F(\varphi_0,q) - E(\varphi_0,q)\right] \ , \tag{7.29}$$

where

$$q = \frac{2t}{\sqrt{\varepsilon_0^2+4t^2}} \ . \tag{7.30}$$

The energy of the system is $E_{tJ} = \langle\Psi|H_{tJ}|\Psi\rangle$ and the energy per site $\varepsilon_{tJ} = E_{tJ}/L$ is still given by Eq. (7.16), but now the kinetic energy of the spinless fermions per site is

$$\varepsilon_{\rm SF}(n) = 2t\langle c_0^\dagger c_1\rangle' - \frac{1}{2}(\langle c_0^\dagger c_0\rangle' - \langle c_1^\dagger c_1\rangle') = -\frac{\sqrt{\varepsilon_0^2+4t_2}}{\pi}E(\varphi_0,q) \ , \tag{7.31}$$

where we have used Eqs. (7.27) and (7.29). For the effective exchange coupling we get

$$J_{\rm eff} = J\left[\langle n_0n_1\rangle' - \frac{1}{2}\left(\langle c_0^\dagger c_1^\dagger c_1c_2\rangle' + \langle c_1^\dagger c_2^\dagger c_2c_3\rangle'\right)\right] = \frac{4t^2}{U}\left\{n^2 - n\frac{\sin 2\pi n}{2\pi} - \frac{\varepsilon_0^2}{2\pi^2t^2}F(\varphi_0,q)\left[F(\varphi_0,q) - E(\varphi_0,q)\right]\right\} , \tag{7.32}$$

where we have used Wick's theorem, namely,

$$\begin{aligned}\langle n_0n_1\rangle' &= n_0n_1 - \langle c_0^\dagger c_1\rangle'^2 \ ,\\ \langle c_0^\dagger c_1^\dagger c_1c_2\rangle' &= n_1\langle c_0^\dagger c_2\rangle' - \langle c_0^\dagger c_1\rangle'^2 \ ,\\ \langle c_1^\dagger c_2^\dagger c_2c_3\rangle' &= n_0\langle c_1^\dagger c_3\rangle' - \langle c_0^\dagger c_1\rangle'^2 \ ,\end{aligned} \tag{7.33}$$

and

$$\begin{aligned}\langle n_0n_1\rangle' - \frac{1}{2}\left(\langle c_0^\dagger c_1^\dagger c_1c_2\rangle' + \langle c_1^\dagger c_2^\dagger c_2c_3\rangle'\right) &= n_0n_1 - \frac{1}{2}(n_1\langle c_0^\dagger c_2\rangle' + n_0\langle c_1^\dagger c_3\rangle')\\ &= n^2 - n\frac{\sin 2\pi n}{2\pi} - I_0(I_0 - I_2) \ .\end{aligned} \tag{7.34}$$

For $n = 1/2$, we get

$$J_{\rm eff} = \frac{1}{U}\left\{t^2 - \frac{2\varepsilon_0^2}{\pi^2}K(q)\left[K(q) - E(\pi/2,q)\right]\right\} \ . \tag{7.35}$$

The gap, using Eq. (7.19), is

$$\Delta_c = 2\varepsilon_0\left\{1 - \frac{2\ln 2}{\pi}\frac{\sqrt{\varepsilon_0^2+4t^2}}{U} \times\left[(1+q^2)K(q) - E(\pi/2,q)\right]\right\} \tag{7.36}$$

and in the small dimerization limit it is given by

$$\Delta_c = 2\varepsilon_0\left[1 - \frac{4\ln 2}{\pi}\frac{\sqrt{\varepsilon_0^2+4t^2}}{U}\ln\frac{4\sqrt{\varepsilon_0^2+4t^2}}{\varepsilon_0}\right] \ . \tag{7.37}$$

If we parametrize the gap in this limit with Δ_D and W, we can see that it is identical to Eq. (7.23).

ACKNOWLEDGMENTS

We would like to thank D. Baeriswyl, H. Beck, E. Jekelman, T. M. Rice, J. Sólyom, and A. Zawadowski for stimulating discussions. One of the authors (K.P.) acknowledges the financial support of the Swiss National Foundation, Grants Nos. 20-33964.92 and 2000-037653.93/1.

* On leave from Research Institute for Solid State Physics, Budapest, Hungary.

[1] For an early review, see D. Jérôme and H. Schulz, Adv. Phys. **31**, 299 (1982); see also Y. Firsov, V. Prigodin, and C. Seidel, Phys. Rep. **126**, 245 (1985).

[2] See B. Gallois *et al.*, Acta Crystallogr. Sect. B **42**, 564 (1986), and reference therein.

[3] L. Ducasse *et al.*, J. Phys. C **19**, 3805 (1986).

[4] Ch. Kröhnke, V. Engelmann, and G. Wegner, Angew. Chem. **92**, 941 (1980); for a recent review of the one-dimensional porperties of these salts, see P. Wzietek *et al.*, J. Phys. I **3**, 171 (1993), and references therein.
[5] G. Sachs, E. Dormann, and M. Schwoerer, Solid State Commun. **53**, 73 (1985).
[6] J.-P. Pouget (private communication).
[7] A. Sudbø *et al.*, Phys. Rev. Lett. **70**, 978 (1993).
[8] G. Japaridze, D. Khomskii, and E. Müller Hartmann, Ann. Phys. (Leipzig) **2**, 38 (1993).
[9] J. Sólyom, Adv. Phys. **28**, 201 (1979).
[10] V. J. Emery, in *Highly Conducting One-Dimensional Solids*, edited by J. T. Devreese, R. P. Edvard, and V. E. van Doren (Plenum, New York, 1979), p. 1221.
[11] E. H. Lieb and F. Y. Wu, Phys. Rev. Lett. **20**, 1445 (1968).
[12] K. Penc and F. Mila, J. Phys. (Paris) Colloq. **4**, C2-155 (1993).
[13] C. M. Bender and S. A. Orszag, *Advanced Numerical Methods for Scientists and Engineers* (McGraw-Hill, New York, 1987).
[14] O. Golinelli, Th. Jolicoeur, and R. Lacaze, Phys. Rev. B **45**, 9798 (1992).
[15] Chr. Seidel and V. N. Prigodin, J. Phys. (Paris) Lett. **44**, L403 (1983).
[16] A. I. Larkin and J. Sak, Phys. Rev. Lett. **39**, 1025 (1977).
[17] S. Barisic and S. Brazovskii, in *Recent Developments in Condensed Matter Physics*, edited by J. T. Devreese (Plenum, New York, 1981), Vol. 1, p. 327.
[18] A. Luther, Phys. Rev. B **14**, 2153 (1976).
[19] H. Shiba and M. Ogata, Int. J. Mod. Phys. B **5**, 31 (1991); M. Ogata and H. Shiba, Phys. Rev. B **41**, 2326 (1990); T. Pruschke and H. Shiba, *ibid.* **44**, 205 (1991).
[20] R. B. Griffiths, Phys. Rev. **133**, A768 (1964).